

p. 99: Several lines were deleted at the bottom of the page. The last sentence should read as follows: "In Eqs. (2) and (3) delete the subscript 1; these quantities then become functions of x . Two additional relations are required to permit a complete solution. They are . . .".

p. 102: Equation (11). Replace K_n by K_p , in both parts.

p. 103: Equation (19). Delete the [1+] from the bracket in the right member. The equation should read

$$\left(\frac{\partial \alpha_c}{\partial T}\right)_p = \frac{p}{2} \frac{\alpha_c^3}{RT^2 K_n} \left[\frac{\Delta H^0}{RT}\right].$$

p. 104: Middle of page—an extra sentence was inserted. Delete the statement just above Eq. (23) . . . "The steady state condition (valid at each position x along the stream line),"

p. 106: In the first line, replace t_0 by T_0 . Equation (30) delete the [1+] from the first bracket in the second term of the right member.

p. 108: Figure 4. Delete the entire bracket in the lower equation for C_p'' . That equation should read

$$C_p'' = \frac{2p}{K_p} \frac{\Delta H^0}{RT^2} \alpha_c^3.$$

The curves in this figure are correct.

p. 108: Figure 5. All the curves in this figure, except the one labeled p_2 , are essentially correct. The numerical magnitude of p_2 was obtained by taking a difference between large quantities (Eqs. (30), (32)). It is regrettable that the latter were not carried to a sufficient number of significant figures in a self-consistent procedure. Also, use of an inconsistent set of symbols introduced further errors. Hence the values for p_2 indicated in Fig. 5 are much too large.

p. 109. As a consequence of the above error, two statements on this page are incorrect.

Delete from the text the last sentence in the first paragraph, which starts with the words, "The rather unexpected . . ."

Also, delete the paragraph marked (b), and insert instead: "It should not prove difficult to distinguish between heat capacity lag due to vibration alone, to dissociation alone, and to dissociation plus vibration. The computed magnitudes of the maximum pressure defects for the $\text{NO}_2-\text{N}_2\text{O}_4$ reaction, for the last two cases are 1.2×10^{-3} atmos and 5.6×10^{-3} atmos, respectively. Since the lag in dissociation cannot be less than the lag in vibrational equilibration involving the bond being broken, study of the pressure defect as a function of nozzle length and impact tube diameter will show two regions, if these are resolvable. Starting with a short characteristic time constant for the apparatus, and proceeding to the longer ones, the case where both reaction and vibration lag will be encountered first and then the case where reaction only lags."

p. 114: Delete the last two sentences on this page.

Comment on the method of solution by successive approximation (p. 105):

Although the proposed procedure for solving the three simultaneous differential equations by successive approximations is entirely feasible, it appears to be very lengthy and involved from the point of view of analyzing numerically appreciable amounts of experimental data. We have now set up a much simpler procedure, in which relaxation theory is utilized. Approximations are thus inherently introduced, but these may be justified in terms of our limiting experimental errors. Details of the experimental pro-

cedures, data on the $\text{NO}_2-\text{N}_2\text{O}_4$ reaction, and their analysis in terms of characteristic relaxation times will be shortly submitted for publication. This research has been supported, in part, by the U. S. Office of Naval Research.

¹ *L. Farkas Memorial Volume*, Research Council of Israel, Special publication No. 1 (Jerusalem, 1952), p. 95 ff

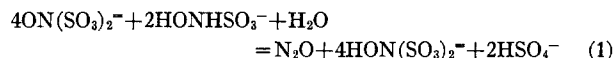
The Iron Catalyzed Reaction between Nitrosyl Disulfonate and Hydroxylamine Monosulfonate Ions

WILLIAM J. RAMSEY AND DON M. YOST
Gates and Crellin Laboratories of Chemistry, California Institute of Technology, Pasadena, California

(Received February 17, 1953)

POTASSIUM nitrosyl disulfonate, $\text{K}_2\text{NO}(\text{SO}_3)_2$, is noteworthy because the solid salt is orange in color and diamagnetic while its neutral aqueous solutions are purple in color and paramagnetic. These neutral solutions hydrolyze slowly to form N_2O and hydroxylamine sulfonates; on the addition of acid the rate of hydrolysis is markedly increased. The mechanism of the hydrolytic reaction is unexpectedly complex as was found by Murib and Ritter¹ and, independently, by us. In order to obtain a more comprehensive picture of the mechanism of the hydrolytic reaction we have explored additional reactions which may play a part in the hydrolysis.

We have found in particular that the reaction in aqueous solution between nitrosyl disulfonate and hydroxylamine monosulfonate ion, $\text{ON}(\text{SO}_3)_2^-$ and HONHSO_3^- , respectively, is catalyzed by iron salts. The reaction is of interest for two reasons. First, very small concentrations of iron cause the reaction to proceed at an easily measurable rate. Second, the rate of the catalyzed reaction is dependent upon hydrogen ion concentration in a way that indicates that predominantly one of the hydrolyzed species of iron (III), $\text{Fe}(\text{OH})^{++}$, is responsible for the catalysis. The stoichiometry of the iron catalyzed reaction is represented by the equation,



Rates of disappearance of nitrosyl disulfonate ion were measured spectrophotometrically (by means of a Beckman Model DU spectrophotometer) under the following initial conditions: Perchloric acid concentration, between 2.5×10^{-4} and 2.5×10^{-3} *VF* (formula weights per liter of solution); ferric perchlorate concentration, as high as 1.46×10^{-6} *VF*; sodium hydroxylamine monosulfonate concentration, between 1.03 and 4.59×10^{-5} *VF*; potassium nitrosyl disulfonate concentration, between 1.4 and 4.7×10^{-6} *VF*; various concentrations of potassium perchlorate and lanthanum perchlorate to adjust the ionic strength; and at temperatures of 20.00 ± 0.03 and $30.00 \pm 0.03^\circ\text{C}$. The details of this investigation are to be published at a later date.

In the majority of cases only the initial rate of disappearance of nitrosyl disulfonate ion was measured, because as the reaction proceeds, side reactions become important.

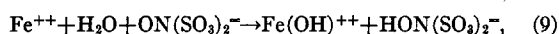
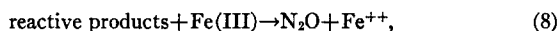
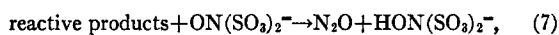
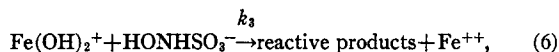
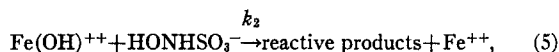
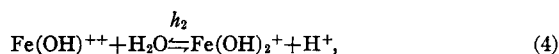
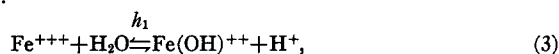
At a given hydrogen ion concentration, temperature, and ionic strength, and at iron concentrations less than 3.5×10^{-7} *VF*, the rate of disappearance of nitrosyl disulfonate ion is well represented by the equation

$$-\frac{d(\text{ON}(\text{SO}_3)_2^-)}{dt} = k_0(\Sigma\text{Fe}^{+3})(\text{HONHSO}_3^-), \quad (2)$$

where (ΣFe^{+3}) represents the total concentration of iron in the reaction solution.

The value of k_0 increases with increasing hydrogen ion concentration up to a value of 1.4×10^{-3} *VF* and then decreases with increasing hydrogen ion concentration.

The following mechanism is in accord with the experimental data:



where h_1 and h_2 are the first and second hydrolysis constants for iron (III), and k_2 and k_3 are the specific rate constants for the reactions represented by Eqs. (5) and (6). Equation (8) summarizes the reactions which may take place between the various species of iron (III) and the reactive products of the initial oxidation of hydroxylamine monosulfonate ion. The reactions represented by Eqs. (9) and either (7), (8), or both must be fast compared to those represented by Eqs. (5) and (6). The rate of disappearance of nitrosyl disulfonate ion under the conditions stated above is then described by the equation

$$-\frac{d(\text{ON}(\text{SO}_3)_2^-)}{dt} = 2 \left\{ \frac{k_2 h_1 (\text{H}^+) + k_3 h_1 h_2}{(\text{H}^+)^2 + h_1 (\text{H}^+) + h_1 h_2} \right\} \times (\sum \text{Fe}^{+3})(\text{HONHSO}_3^-). \quad (10)$$

The value for the constant h_1 was taken from the work of Siddall and Vosburgh.²

The values obtained for h_2 , k_2 , and k_3 at a temperature of 20°C and at an ionic strength of 2.6×10^{-2} are $7 \times 10^{-4} \text{ mole} \cdot \text{l}^{-1}$, $13.9 \pm 1.4 \times 10^4 \text{ l} \cdot \text{mole}^{-1} \cdot \text{min}^{-1}$, and $1.5 \pm 0.2 \times 10^4 \text{ l} \cdot \text{mole}^{-1} \cdot \text{min}^{-1}$, respectively.

We are indebted to the Research Corporation, the Shell Oil Company, and E. I. du Pont de Nemours and Company for grants which supported this research.

¹ J. H. Murib and D. M. Ritter, *J. Am. Chem. Soc.* **74**, 3394 (1952)

² T. H. Siddall, III, and W. C. Vosburgh, *J. Am. Chem. Soc.* **73**, 4270 (1951)

The Forces between Hydrogen Molecules

ARTHUR A. EVETT AND HENRY MARGENAU
Yale University, New Haven, Connecticut
(Received March 2, 1953)

EARLIER calculations of the H_2 - H_2 interaction,¹ based on the use of screening-constant functions, seemed to lead to reasonable answers only with the use of a nuclear charge much greater than the correct value for the isolated molecule, $Z_0 = 1.166$. The present work is a recalculation of the exchange forces for $Z = Z_0$. A small numerical error in the earlier work is eliminated and the exchange energy, instead of being slightly negative as reported previously, is actually positive. This removes all perplexing features from the problem and yields results in substantial agreement with experiments.

The total interaction, consisting of exchange, van der Waals, and quadrupole energies, is plotted for different relative orientations of the molecules in Fig. 1.

These orientations are:

Case (a): Both molecular axes are parallel to R , the line joining the centers.

Case (b): One axis is parallel, the other perpendicular to R .

Case (c): Both axes are perpendicular to R and parallel to each other.

Case (d): Both axes are perpendicular to R and perpendicular to each other. Case (d) was not treated in the earlier paper.

A weighted average over all orientations is shown in Fig. 2 and is compared with the semi-empirical curve of Hirschfelder, Bird, and Spotz,² which was derived by fitting viscosity data. The work of De Boer and Michels,³ based on an evaluation of second virial coefficients, leads to points slightly lower than Hirschfelder's.

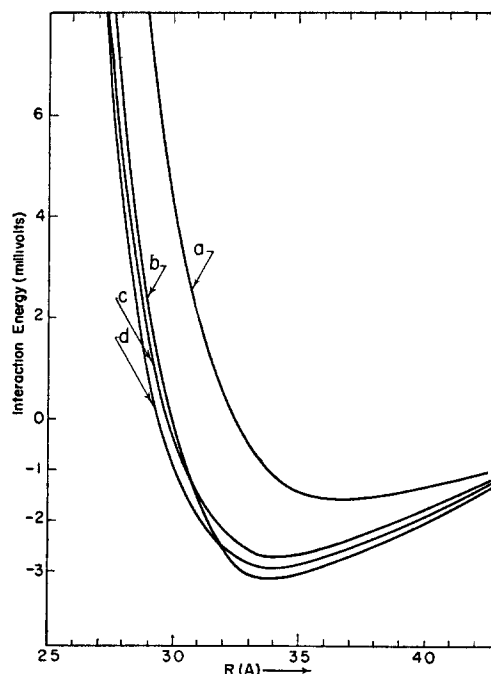


FIG. 1. Total energy of interaction for different molecular orientations as function of intermolecular distance

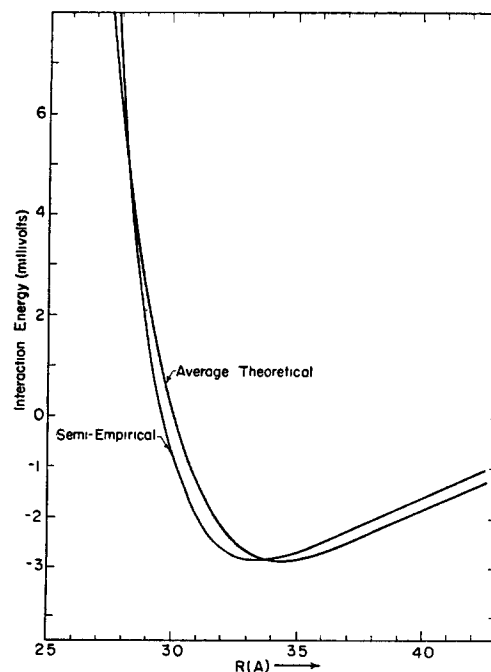


FIG. 2. Comparison of theoretical interaction (averaged over molecular orientations) with empirical curve of Hirschfelder, Bird, and Spotz.